Composition of the Primary Cosmic Radiation at $\lambda = 10°$ N†

G. W. McCLURE
Bartol Research Foundation of The Franklin Institute, Swarthmore, Pennsylvania
(Received August 9, 1954)

A balloon-borne instrument comprising a fast ionization chamber interposed in a G-M counter train has been flown near the geomagnetic equator for the purpose of determining the fluxes of protons and He nuclei in the primary cosmic radiation. The apparatus measures the specific ionization of each particle that traverses the telescope, and contains a shower detector to aid in the identification of multiple-particle events of either local or external origin. Under the assumption that all telescope coincidences resulted from particles incident within the counter-defined solid angle, the total vertical flux, extrapolated to the "top of the atmosphere," is $I_{\text{total}}=260$ sterad^{-1} m^{-2} sec^{-1}. The "top"-extrapolated fluxes of primary protons and He nuclei deduced from the ionization distributions recorded at various depths (17 g/cm^2 and greater) are as follows: $I_{\text{H}}<145$ sterad^{-1} m^{-2} sec^{-1}; $I_{\text{He}}<38$ sterad^{-1} m^{-2} sec^{-1}. The large difference between I_{total} and $(I_{\text{H}}+I_{\text{He}})_{\max}$ is believed to arise from air showers and/or nuclear events produced by particles incident from outside the telescope solid angle. The consequences of neglecting these spurious effects in interpretating counter-telescope measurements are discussed with particular reference to influences on the deduced form of the primary-proton energy spectrum, and the total energy flux associated with the primary radiation.

I. INTRODUCTION

THE primary cosmic radiation is believed to consist of protons, α particles and heavier nuclei roughly in the intensity ratio 85:15:1. While the protons are the most abundant component above the atmosphere, the heavier particles split up in atmospheric collisions yielding a total flux of proton and neutron fragments comparable to the primary proton flux at depths of the order of 40 g/cm^2. Because of their relatively large flux, the He nuclei play an especially important role in the atmospheric production of secondaries. In addition to contributing to our understanding of the cascade development of the cosmic radiation, knowledge of the absolute flux and energy spectrum of the primary α-particles may assist materially in establishing the origin of cosmic rays.

The α-particle flux has been measured at a number of latitudes by means of various devices including low-pressure G-M counters,[1–3] photographic emulsions,[4,5] scintillation counters,[6] proportional counters,[7,8] Čerenkov detectors,[9] and a combination cloud chamber, Čerenkov detector.[10] In general, the precision of the measurements has left much to be desired owing partly to large statistical uncertainties and partly to difficulties encountered in the interpretation of the experimental data.

The present work describes the results of an α-flux measurement conducted near the geomagnetic equator with an instrument which incorporates the best features of several of the methods employed earlier by other investigators. The method is similar in principle to that used by Perlow at $\lambda=41°$ but utilizes a high-pressure ionization chamber instead of proportional counters to ascertain the specific ionization of individual incoming particles. The present method has no fundamental superiority over the proportional-counter method, but provides ionization resolution and stability equivalent to that of Perlow's arrangement with much simpler electronics.

An earlier form of the ion chamber instrument was designed for use in a cosmic-ray survey conducted in India in 1952–53.[11] Owing to time limitations and the small load-carrying capacity of the balloons available, it was necessary to make several sacrifices in the original design. The present refined version of the instrument overcomes many of the earlier inadequacies by including a pulse-height recorder and a multi-counter shower detector to aid in the identification of showers and other multiple-particle events which can yield ionization pulses of the same size as those produced by α particles.

With these refinements there still remains some ambiguity as to the identification of α-particle events, however it is possible to obtain with the instrument in its present form upper limits on both the primary proton and He intensities which probably do not differ appreciably from the true fluxes. In addition some important conclusions regarding the seriousness of spurious telescope-triggering events are obtained. Inasmuch as the present proton-flux upper limit is substantially lower than values deduced from earlier G-M counter measurements, the proton data are perhaps the most interesting aspect of the experimental results.

† Assisted by the joint program of the U. S. Office of Naval Research and the U. S. Atomic Energy Commission.

[1] S. F. Singer, Phys. Rev. **76**, 701 (1949).
[2] M. A. Pomerantz and F. L. Hereford, Phys. Rev. **76**, 997 (1949).
[3] S. F. Singer, Phys. Rev. **80**, 47 (1950).
[4] Goldfarb, Bradt, and Peters, Phys. Rev. **77**, 751 (1950).
[5] B. Peters, *Progress in Cosmic Ray Physics* (North Holland Publishing Company, Amsterdam, 1952), Vol. 1, Chap. IV.
[6] E. P. Ney and D. M. Thon, Phys. Rev. **81**, 1069 (1951).
[7] Perlow, Davis, Kissinger, and Shipman, Phys. Rev. **88**, 321 (1952).
[8] Davis, Caulk, and Johnson, Phys. Rev. **91**, 431 (1953).
[9] J. R. Winckler and K. Anderson, Phys. Rev. **93**, 596 (1954).
[10] J. Lindsley, Phys. Rev. **93**, 899 (1954).
[11] M. A. Pomerantz, J. Franklin Inst. (to be published).

II. DESCRIPTION OF THE APPARATUS

A diagram of the counter telescope is shown in Fig. 1. The four counters C_1, C_2, C_3, and C_4 (glass walls, Aquadag cathodes, effective dimensions 17.8 cm×3 cm) define the acceptance solid-angle of the instrument. The basic requirement for an event to be recorded is that these counters be discharged in coincidence. The tray S serves as a shower detector and functions as such whenever two or more of the seven counters it contains are discharged in coincidence with $C_1C_2C_3C_4$. Owing to the thickness of the counter envelopes, adjacent counters of tray S have spaces of approximately 1.6 mm between their internal "active" volumes. All counters contain a mixture composed of 86 percent argon and 14 percent butane at a total pressure of 100 mm Hg.

The ionization chamber is of the fast, electron-collection variety, filled with 99.9 percent pure argon at a pressure of 300 psi. Internal constructional details are the same as those of an earlier design described elsewhere.[12] Pulses from a calibration Po-α source built into the ion chamber wall (operative only during ground tests) reach voltage saturation at a cathode potential of 800 volts. A single 1000-volt battery operates the ion chamber in the region of pulse-height saturation and supplies the proper operating potential for the G-M counters.

The general arrangement of the electronics is indicated in the block diagram, Fig. 2. Each quadruple coincidence $C_1C_2C_3C_4$ (10-μsec resolving time) intensifies for 50 μsec the "spot" on the screen of a 3-inch cathode-ray tube, (C.R.T.), and triggers simultaneously a sweep circuit which generates a linear "sawtooth" wave form. The amplified ionization chamber pulse causes a vertical deflection of the C.R.T. spot proportional to the ionization of the particle initiating the main fourfold coincidence. When no shower is detected, the sweep sawtooth is allowed to pass the clamping circuit and a voltage *vs* time oscilloscope presentation of the ion-chamber pulse results. When two or more counters of tray S are discharged simultaneously with $C_1C_2C_3C_4$, indicating a multiple-particle or "shower" event, the clamping circuit prevents the sawtooth pulse from reaching the horizontal deflection plates and the ion-chamber pulse appears on the C.R.T. as a vertical "spike" with no horizontal extension. Thus, events accompanied by showers are clearly distinguished from those in which no shower is detected. All pulses appearing on the C.R.T. screen are recorded on a continuously moving 16-mm photographic film.

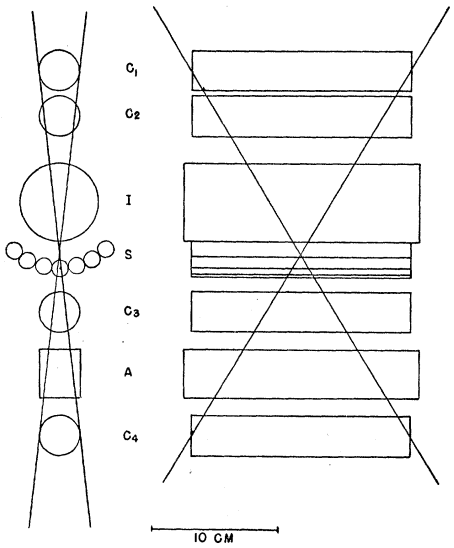

FIG. 1. Diagram of counter telescope. C_1, C_2, C_3, C_4—G-M counters. S-shower tray containing seven G-M counters. I-electron collection ionization chamber. A—4 cm Pb absorber.

The ion-chamber linear amplifier comprises three stages with 0.025 percent inverse feedback and has an over-all gain of 4000. The frequency band width of the amplifier is adjusted to provide the best signal to noise ratio consistent with the accurate preservation of the ion-chamber pulse shape. The rise time of the chamber pulses as viewed at the amplifier output is 10 μsec and the decay time about 100 μsec. Through selection of the (6AK5) amplifier input tube it was possible to attain an amplifier noise level less than one-tenth the average amplitude of the pulses produced by sea-level mesons.

The output pulses from the linear amplifier are fed into a push-pull output stage which provides additional amplification required to drive the oscilloscope. The 10-μsec delay-line between the linear amplifier and scope amplifier allows the horizontal sweep and intensifier circuits to start before the ion-chamber pulse arrives at the vertical deflection plates. This delay provides a clearly-defined base line for each pulse, eliminating any difficulty that might arise from low-frequency amplifier microphonics or gradual drift of the quiescent position of the oscilloscope spot. In a shower event, where the horizontal sweep does not operate, the base of the ion-chamber pulse is marked by a bright spot where the intensified oscilloscope beam rests for several μsec prior to the onset of the pulse.

The set of instruments surrounding the screen of the C.R.T. includes a thermometer, a clock, and a mercury manometer. The manometer indicates atmospheric pressure to within ±0.5 mm in the range 0–70 mm Hg. Readings of these instruments are recorded on the film by momentary scale illumination at 5-minute time intervals. One-minute time markers also appear on the film record. An aneroid barometric switch attached to the outside of the flight gondola operates a light near the oscilloscope, marking the film at predetermined pressure-intervals in the range of altitudes below the operating threshold of the 70-mm manometer. In this

[12] M. A. Pomerantz and G. W. McClure, Phys. Rev. 86, 536 (1952).

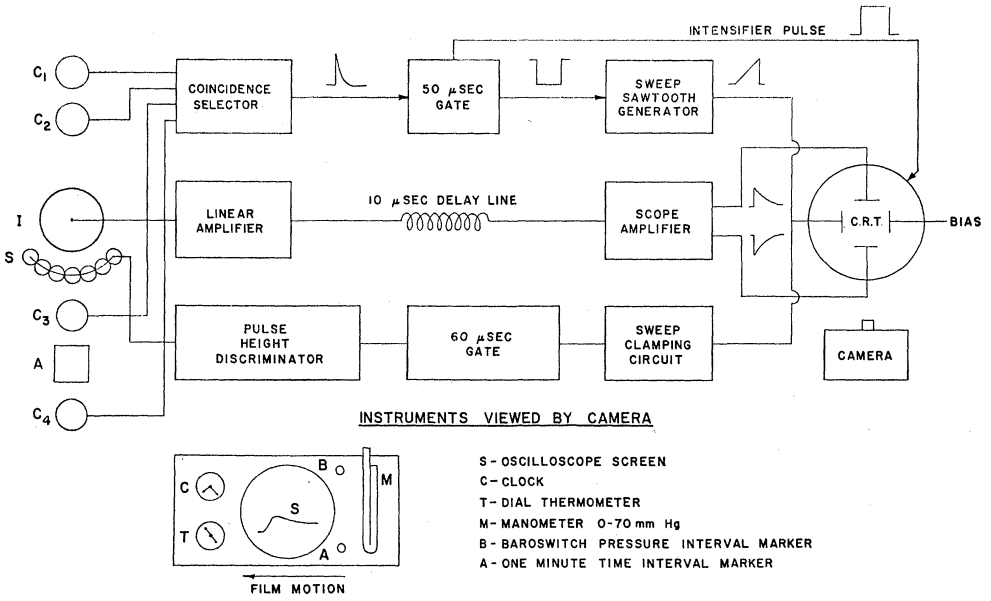

FIG. 2. Circuit block-diagram and arrangement of instruments viewed by camera.

manner, a complete time-altitude record directly correlated with the cosmic-ray pulses is obtained at all altitudes.

The 4-cm Pb absorber interposed in the telescope at position A is intended to prevent the triggering of the instrument by slow protons whose specific ionization is such as to cause confusion with relativistic α-particle events.

The entire apparatus including the oscilloscope and camera recorder is contained in a 24-in. diameter aluminum sphere sealed at 1 atmosphere in order to eliminate high voltage corona troubles, and to preserve the film record in cases where the instrument might land on water. In flight the gondola is wrapped in three loosely-fitting pliofilm bags to provide warmth by the "greenhouse" effect.

III. SEA-LEVEL TESTS

A preliminary account of sea-level results obtained with the present type of ion chamber mounted in a modified form of G-M counter train has been published previously.[13] Results obtained with the actual balloon-borne apparatus at $\lambda=52°$ are shown in Fig. 3. In order to simulate actual flight conditions as nearly as possible, a battery pack identical to that used in flight was employed in the ground tests. The shapes and heights of the pulses were ascertained by projection of the film record on the screen of a 16-mm film editor. Within statistical uncertainties, the pulse-height distributions obtained in the first and final halves of the 445-min. run analyzed in Fig. 3 were identical. The excellent stability of the instrument against battery strength depletion is indicated by the fact that the average pulse height during the two time intervals differed by less than 2 percent.

[13] G. W. McClure, Phys. Rev. **87**, 680 (1952).

The pulse height $h=6.1$ in the scale of Fig. 3 and all subsequent data presentations corresponds approximately to the most probable ionization of the cosmic rays at sea level. The distribution of pulse heights above and below the peak is attributable to: (1) statistical fluctuations in gas ionization arising from the finite number and large energy spread of the primary knock-on electrons;[14,15] (2) inhomogeneity of energy and particle composition of the incident radiation; (3) variation in path length of particles traversing the ion chamber; and (4) experimental uncertainties in the measurement of pulse height.

Neglecting (3) and (4), which have a minor broadening effect, we have calculated the shape of the pulse height distribution to be expected on the basis of the Symon theory of energy-loss fluctuations[15] and the sea-level meson spectrum of Wilson.[16] The smooth curve in Fig. 3 represents the calculated distribution.

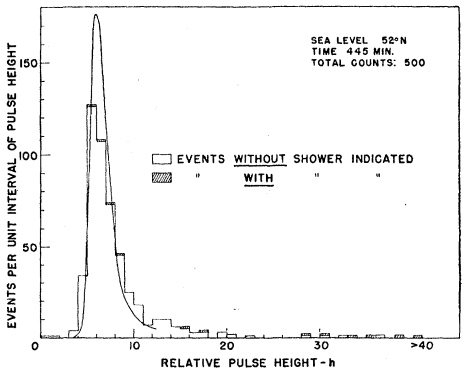

FIG. 3. Sea level differential pulse-height distribution ($\lambda=52°$ N).

[14] L. Landau, J. Phys. (U.S.S.R.) **8**, 201 (1944).
[15] K. R. Symon, thesis, Harvard University, 1948 (unpublished).
[16] J. G. Wilson, Nature **158**, 414 (1946).

The curve is plotted so that its peak matches the maximum of the histogram and so that areas under the curve and the histogram are equal in the interval $0<h<12$. The calculated most probable energy loss of the mesons in the ion chamber is 0.272 Mev, and the relationship between pulse height, h, and energy loss, E (in Mev), established by the abscissa normalization is $h=22.5E$.

The fact that the width (at half-maximum) of the histogram is greater by about one h-unit than that of the calculated distribution may well be entirely a consequence of experimental uncertainty in the pulse-height determination. The width of the oscilloscope trace and the amplitude of the noise are such that errors of the order of $\Delta h=\pm 1.0$ are expected to occur in the pulse-height measurements. An additional broadening of the order of 5 percent can be attributed to the variation in ion-chamber path length of the incident particles.

On the basis of the computations, the expected fraction of pulses exceeding twice the most probable pulse height (i.e., $h=12$) should be less than one percent. The number of events with $h>12$ actually observed is 11 percent of the total. Of these, about one-third (mostly shower-accompanied) are larger than $h=20$. The larger size of the histogram "tail" can neither be attributed to errors in pulse-height measurement, nor to geometrical effects, and is believed to arise in part from electrons knocked out of the chamber walls by the incoming mesons—roughly 9 percent of the mesons should be accompanied by such knock-ons[17,18]—and partly from approximations made in our selection of fluctuation-function parameters. (We assumed that the maximum energy transferred to a secondary electron in the gas is equal to the value 0.3 Mev, for which the electron range in the argon equals the radius of the chamber. In so doing we attempted to compensate roughly for the energy "lost" by long range secondaries which are produced in the gas and stop in the chamber walls. According to the knock-on theory,[19] about 5 percent of the sea-level mesons produce one or more secondaries in the gas whose energy exceeds the assumed 0.3-Mev cutoff. These neglected mesons yield a pulse-height distribution with a peak occurring at about $h=12$ and contribute about two-thirds of their pulses to the region above $h=12$.)

The events with $h>20$ are much more heavily shower accompanied than those with $h<20$. Inasmuch as the fraction of mesons yielding secondaries in the gas which can reach the shower tray is completely negligible, the probability of shower accompaniment should be independent of the size of the ionization pulse. The larger shower pulses are therefore believed to arise from cosmic-ray electrons rather than from mesons. Subtraction of the shower events from the pulse height interval $h>20$ leaves a residual tail whose area is roughly equal to 1 percent of the total histogram area, and which presumably represents the high end of the meson pulse-height distribution.

The theory of electron knock-on production[19] indicates that aside from effects introduced by local nuclear interactions, the sea-level mesons and primary protons near the geomagnetic equator should yield practically identical pulse-height distributions. Hence, the sea-level data play an important role in the analysis of the balloon-flight results.

IV. THEORETICAL CHARACTERISTICS OF THE INSTRUMENT

In Fig. 4 are plotted the calculated integral pulse-height distributions for monoenergetic particles having several particular values of p/mc pertinent to the discussion of the sea-level and high-altitude measurements. As the horizontal separations between the integral distributions for singly-charged particles ($z=1$) having $p/mc=1$, 10, 100, and 1000 are comparable to the experimental pulse-height resolution, the instrument cannot be expected to yield detailed information on energy spectra of relativistic particles.

The manner in which the tail of the theoretical distribution for monoenergetic particles with $p/mc\approx 10$ must be modified in accordance with the sea-level observations is indicated by the dot-dash curve. (The sea-level momentum spectrum is peaked at $p/mc\simeq 18$ and all but a few percent of the mesons belong to the interval $2<p/mc<200$.) Also shown is the calculated distribution for primary alpha particles having momenta equal to the geomagnetic cutoff in the vertical direction at $\lambda=10°$ ($p/mc\simeq 7$). It is evident from inspection of these curves that relativistic protons and π mesons which traverse the ion chamber unaccompanied by secondaries from nuclear events contribute practically no pulses above the pulse-height threshold for relativistic α particles.

The curves labeled P and P' are the integral pulse-height distributions for the lowest energy protons (208 Mev) which can penetrate the telescope material. The former is the limiting curve for protons which enter from above the telescope moving downward, and the latter for those which enter from below proceeding

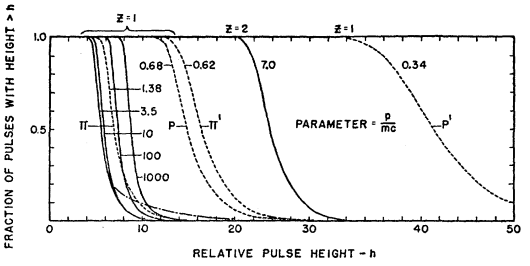

FIG. 4. Calculated integral pulse-height distributions for singly-charged ($Z=1$) and doubly-charged ($Z=2$) particles having various values of parameter p/mc.

[17] Brown, McKay, and Palmatier, Phys. Rev. **76**, 506 (1949).
[18] F. L. Hereford, J. Franklin Inst. **249**, 449 (1950).
[19] H. J. Bhabha, Proc. Roy. Soc. (London) **164**, 257 (1938).

upward. The corresponding curves for the lowest energy π mesons (107 Mev) capable of penetrating the absorber are labeled π and π' respectively. The primed curves P' and π' are displaced to the right of the corresponding unprimed curves, owing to the asymmetrical distribution of stopping material above and below the ion chamber.

V. BALLOON-FLIGHT OBSERVATIONS

Two instruments of the type described were flown in September, 1953 in the vicinity of the Galapagos Islands as one phase of the ONR-sponsored Skyhook balloon expedition designated "Project CHURCHY." Only one of the two instruments was recovered.

The successful flight was launched at 1430 G.M.T. on September 6, ascended at an average rate of 720 ft/min until 1635 G.M.T. and then leveled off at an atmospheric depth of 12.5 to 13 mm Hg for 4.2 hours. The gondola drifted due west while at ceiling altitude, and descended at a point about 400 miles from the launching-site. The time *vs* atmospheric pressure record of the flight obtained independently by General Mills, Inc., agreed within ± 0.5 mm with pressure readings on the film record.

The temperature inside the gondola was 19°C at the beginning of level-off, slowly decreased to a minimum of 4°C after 3 hrs. at altitude and then gradually increased, reaching 8°C at the time of descent. Data recorded during the first and last halves of the period of level flight agreed within statistical uncertainties, giving no indication of adverse effects associated with the temperature variations.

Preflight calibration of the instrument in the field with Po-α particles and sea-level mesons verified that the relationship between pulse height and energy loss was the same as in the sea-level tests described above.

The differential pulse-height distribution recorded during the 255-min level-off period at 12.5–13.0 mm Hg

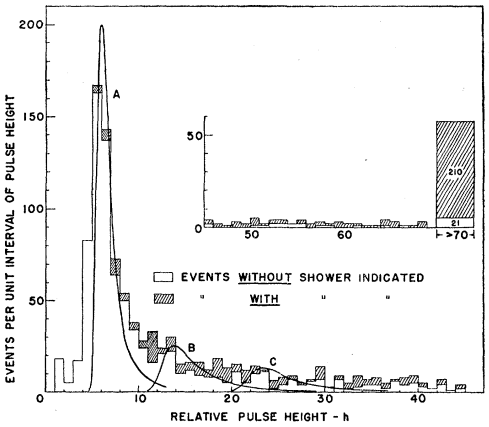

FIG. 5. Differential pulse-height distribution recorded at 12.5–13 mm Hg, $\lambda = 10°$ N (histogram). Curves *A*, *B*, and *C* are calculated pulse-height distribution for primary protons, 208-Mev protons and He nuclei (of geomagnetic cutoff energy) respectively.

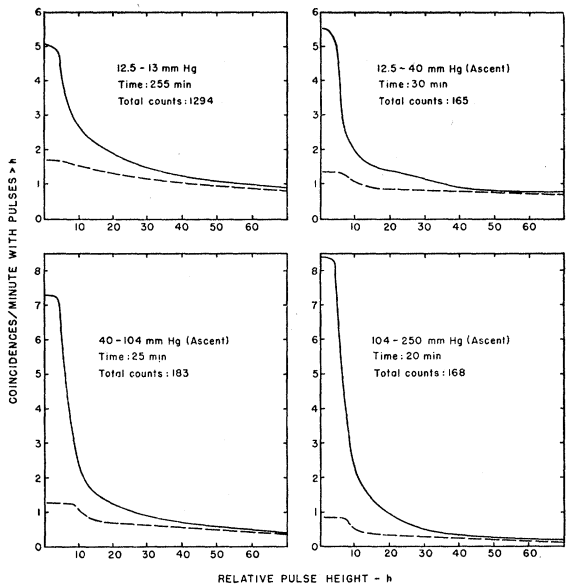

FIG. 6. Integral pulse-height distributions recorded at various altitudes. Smooth curves = total counting rate. Dashed curves = shower counting rate.

is shown in Fig. 5, and integral distributions corresponding to this and three lower altitude intervals traversed during the ascent are plotted in Fig. 6. Numerical data used in the analysis are given in Table I.

Many pulses which saturated the amplifier were recorded. The tops of the saturation pulses appeared below the upper edge of the oscilloscope screen and are clearly visible on the film record, so that few events, if any, could have been overlooked in scanning the film. All pulses are counted in calculating the apparent total flux discussed in the next section, but only those in the range $0 < h < 70$, which are undistorted by the amplifier, are considered in the detailed analysis.

VI. ANALYSIS OF BALLOON-FLIGHT RESULTS

A. Total Flux

Figures 5 and 6 and the last two columns of Table I indicate that a large percentage of the recorded events high altitudes are multiple-particle or "shower" events. It will be shown at the conclusion of the analysis that not all of the showers which occur near the "top of the atmosphere" are caused by local nuclear events produced in the telescope material by single particles incident within the counter-defined solid angle. Nevertheless it is of some interest to compare the "apparent" total intensity—computed with the usual assumption that all counts result from telescope-oriented incident particles—with the results of other investigations in equatorial regions. The pertinent total flux measurements are listed in Table II. The present results for $\lambda = 10°$ agree very closely with prior measurements at $\lambda = 0°$ and 3° as is to be expected from the small

TABLE I. Observed numbers of events in various pulse-height categories *vs* atmospheric pressure. Quantities in parenthesis are corresponding flux values; units sterad^{-1} m^{-2} sec^{-1}.

Atmospheric pressure interval	Time (min)	$0<h<12$ Without shower	$0<h<12$ With shower	$12<h<20$ Without shower	$12<h<20$ With shower	$20<h<48$ Without shower	$20<h<48$ With shower	$48<h<70$ Without shower	$48<h<70$ With shower	$h>70$ Without shower	$h>70$ With shower	Totals Without shower	Totals With shower	With and without
12.5–13.0	255	611 (132)	56 (12)	95 (21)	49 (10.6)	118 (25.5)	81 (17.5)	14 (13)	40 (18.7)	21 (4.5)	209 (45)	859 (186)	435 (94)	1294 (280)
12.5–40	30	104 (190)	9 (17)	5 (9)	5 (9)	13 (24)	5 (9)	0 (0)	1 (2)	2 (4)	21 (39)	124 (228)	41 (75)	165 (303)
40–104	25	126 (278)	10 (22)	14 (31)	2 (4)	10 (22)	8 (18)	0 (0)	3 (7)	1 (2)	9 (20)	151 (332)	32 (71)	183 (403)
104–250	20	127 (350)	8 (22)	14 (39)	1 (3)	8 (22)	3 (8)	1 (3)	2 (6)	1 (3)	3 (8)	151 (415)	17 (47)	168 (462)
Text reference		*A* events		*B* events		*C* events								

(5 percent) change in the vertical cutoff energy between 0° and 10°. The total flux values at $\lambda=18°$ and 20° are all somewhat higher than the 10° values obtained herewith.

There is no evidence that the unusually large amount of material placed near the slides of the counter telescope in the present experiment (70 lb of batteries, electronics, etc.) had an effect upon the telescope counting rate.

B. Relativistic Singly-Charged Particles

By comparing a measured pulse-height distribution with the calculated distribution for a group of incident particles having a pre-determined or assumed energy spectrum, it is possible to deduce an upper limit for the flux of particles in question. In performing such deductions, allowance must be made not only for ionization fluctuations but also for the possibility that the incident particles may undergo nuclear interactions in the telescope material thereby creating events of substantially larger ionization that would otherwise occur. (While the sea-level μ mesons do not give rise to such interactions, the protons, π mesons and α particles present in the high-altitude radiation probably give rise to a large number of locally-produced bursts.)

TABLE II. Total flux values near the equator.

Geomagnetic latitude	Flux of particles sterad^{-1} m^{-2} sec^{-1}	Absorber	Atmospheric depth	Author
0°	270±10	3 cm Pb	15 g/cm^2	[a]
0°	310±10	No Pb	15 g/cm^2	[a]
0°	280±40	No Pb	Rocket	[b]
3°	300±20	4 cm Pb	10 mm Hg	[c]
3°	240±10	4 cm Pb	Top extrapolated	[c]
3°	280±20	7.5 cm Pb	10 mm Hg	[c]
3°	230±10	7.5 cm Pb	Top extrapolated	[c]
10°	280±8	4 cm Pb	13 mm Hg	[d]
10°	260±8	4 cm Pb	Top extrapolated	[d]
18°	390±20	4 cm Pb	10 mm Hg	[c]
18°	350±10	4 cm Pb	Top extrapolated	[c]
18°	360±20	7.5 cm Pb	20 mm Hg	[c]
18°	330±10	7.5 cm Pb	Top extrapolated	[c]
20°	310±10	3.0 cm Pb	15 g/cm^2	[a]

[a] Winckler, Stix, Dwight, and Sabin, Phys. Rev. **79**, 656 (1950).
[b] J. A. Van Allen and S. F. Singer, Phys. Rev. **78**, 819 (1950).
[c] M. A. Pomerantz, Phys. Rev. **95**, 531 (1954).
[d] Present work.

To derive flux-values for the various components, the recorded pulses are broken down into three main groups as follows: (1) Pulses in the interval $0<h<12$ most of which are produced by relativistic singly-charged particles ($E/mc^2>1.0$), (2) Pulses in the interval $12<h<20$ from which an upper limit can be established on the intensity of slow particles likely to interfere with the He flux determination, (3) Pulses in the interval $20<h<48$ from which will be derived an upper limit for the flux of relativistic He nuclei.

The letters *A*, *B*, and *C* denote events in categories (1), (2) and (3) respectively which are *unaccompanied by shower indications*. (Analysis of the shower events on the basis of this particular division of the data is not especially significant because the number of particles which traverse the chamber in any such event is unknown.) The symbols I_A, I_B, and I_C represent the fluxes of particles yielding events of types *A*, *B*, and *C* respectively. Numerical values of these fluxes are listed in Table III.

Using the Symon theory of energy loss fluctuations,[15] the pulse-height distribution of primary protons with an integral energy spectrum of the form $E^{-1.5}$ and a low-energy cutoff of 14 Bev (theoretical geomagnetic cutoff) was calculated. This distribution is superimposed upon the histogram in Fig. 5 (curve *A*). The relationship between calculated energy loss and ion-chamber pulse height used in the abscissa matching is the same as that used in the analysis of the sea-level data. According to the fluctuation theory and the sea-level calibration the *A* events include (1) all but 9 percent of the primary protons which do not undergo nuclear interactions in the telescope material, (2) at least 90 percent of the secondary singly-charged particles with $1.0<E/mc^2<14.0$, which do not interact locally, and (3) some smaller fraction of the secondaries with $0.22<E/mc^2<1.0$. (In the last instance the fraction of pulses contributed to the interval $0<h<12$ is strongly energy-dependent.)

Because of the limited resolution of the instrument

TABLE III. Fluxes I_A, I_B, I_C of particles yielding events of types A, B, and C respectively, and derived flux values as follows: I_A'—intensity of particles with $Z=1$ and $E_{\text{kin}}/mc^2>1.0$ corrected for ionization fluctuation only; I_A''—intensity of same group corrected for maximum effect of local nuclear interactions (upper limit); I_B'—intensity of slow particles—principally protons incident from below with $235<E_{\text{kin}}<348$ (see text); I_C'—intensity of He nuclei corrected only for ionization fluctuation of singly-charged particles. I_C'' intensity of He nuclei corrected for maximum effect of local nuclear interactions (upper limit). See text for further considerations regarding He intensity. Units—sterad^{-1} m^{-2} sec^{-1}.

Atmospheric pressure interval (mm Hg)	I_A	I_A'	I_A''	I_B	I_B'	I_C	I_C'	I_C''	I_{total}
12.5–13.0	132±5	145	210	20.6±2	10±2	25.5±2.5	24	39	280±8
12.5–40	190±19	209	304	9±4	−7±5	24.0±6.7	22	36	303±24
40–104	278±25	306	445	31±8	7±8	22.0±7.0	19	31	403±30
104–250	350±31	385	560	39±10	9±10	22±8.0	18	29	462±36

it is not possible to separate the primaries from either the relativistic or the slow secondaries in the categories (2) and (3). One can, however, derive an upper limit for the flux of particles with $E/mc^2>1.0$ which do not undergo local nuclear interactions by simply attributing all events in the interval $0<h<12$ to particles in categories (1) and (2) and making the indicated (9 percent) allowance for ionization fluctuations. When this correction is applied to the recorded A events one obtains the flux values I_A' listed in Table III. With a further correction for the maximum loss of pulses from the A group which could occur through the production of local nuclear interactions, the flux values I_A'' are obtained.

In calculating I_A'' we assume that every particle which passes within the "geometrical" radius of a nucleus anywhere in the telescope gives rise to a pulse not included in the A group, i.e., either a shower event or an ionization burst with $h>12$. To obtain the "geometrical" collision probabilities, we have used here and elsewhere in this paper cross sections given by the formula

$$\sigma=\pi r_0^2(A_1^{\frac{1}{3}}+A_2^{\frac{1}{3}}-1)^2, \quad r_0=1.38\times10^{-13}\text{ cm}, \quad (1)$$

where A_1 and A_2 are the atomic weights of the incident and target nuclei, respectively. Mean free paths calculated from this expression agree well with the data of Kaplon *et al.*[20] on α-particle and heavy-nucleus collisions in glass and brass, and the formula also gives reasonable values for collision mean free paths of single high-energy nucleons.

In view of the extreme nature of the applied correction for nuclear interactions and the possibility that the A events include some non-relativistic particles, I_A'' must be regarded as a conservative upper limit on the relativistic-particle flux in each altitude range. Comparison of the values I_A'' and I_{total} (plotted as a function of altitude in Fig. 7) yields the conclusion that *at most 75 percent of the telescope counting rate at 12 mm Hg can be attributed to relativistic singly-charged particles, including albedo, incident within the counter-defined solid angle. Extrapolation of the I_A'' and I_{total} curves to zero pressure indicates that at the "top of the atmosphere" the relativistic particle contribution is less than 60 percent of the telescope counting rate.*

It is interesting to note that at 50 mm Hg the calculated curve I_A'' rises above the I_{total} curve. This indicates that the correction of flux I_A' for local nuclear events is excessive, at least for particles encountered at depths greater than 50 mm Hg. Inasmuch as I_A'' exceeds I_{total} by a nearly constant percentage in the two lower altitude intervals, it would appear that the correction referred to above might be in error by approximately the same amount, percentagewise, over the entire range of altitude investigated, including the 12.5–13 mm Hg interval. If this were actually the case, the extrapolated flux of relativistic singly-charged particles at zero pressure would be <120 sterad^{-1} m^{-2} sec^{-1}, or less than half the extrapolated value of I_{total}.

We have attempted to estimate from photographic emulsion data on stars produced by high-energy protons the approximate fraction of proton traversals of the telescope which should give rise to nuclear interactions of the type that yield either a shower indication or an ionization pulse outside of the A interval. Such attempts

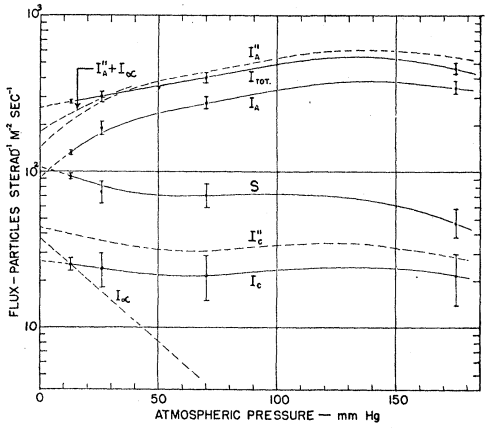

FIG. 7. Altitude variation of several measured and derived particle fluxes. I_A, I_B, I_C=fluxes of particles yielding events of types A, B and C respectively. I_A''=maximum flux of relativistic singly-charged particles (derived from curve I_A by applying corrections for large ionization fluctuations and removal of events from A group by nuclear interactions); I_C''=maximum flux of He nuclei derived from curve I_C; I_α=maximum flux of He nuclei to a more refined approximation (see text); S=effective flux of shower associated particles.

[20] Kaplon, Peters, Reynolds, and Ritson, Phys. Rev. **85**, 295 (1952).

are considered to be of somewhat dubious value since most of the emulsion stars for which the primary-particle energy has been established result from C, N, Ag, and Br collisions, whereas nearly all of the proton interactions in the counter telescope occur in the Pb absorber. The manner in which the multiplicity, energy distribution, and angular distribution of secondaries varies with the atomic weight of the struck nucleus, is as yet not completely known.

Finally it should be emphasized that the instrument is incapable of distinguishing between particles incident from the 0° and 180° zenith angles, so that the relativistic particle flux may include a substantial albedo contribution. The measurements of Anderson and Winckler[21] at $\lambda=10°$N (Čerenkov detector) indicate that the flux of relativistic singly-charged albedo amounts to approximately 15 percent of the total intensity. This would imply an albedo flux of approximately 40 sterad^{-1} m^{-2} sec^{-1} and would reduce our estimate of the primary proton flux to <100 sterad^{-1} m^{-2} sec^{-1}.

C. Slow Protons and π Mesons

In this section we attempt to estimate the flux of slow singly-charged particles capable of yielding ionization pulses of the same size as those produced by primary He nuclei. To obtain such an estimate we examine the slow-particle contribution to the recorded B events, i.e., events unaccompanied by shower indications with pulse-heights in the interval $12<h<20$. (The total flux of particles yielding this type of event is designated I_B, and is given for each altitude interval in Table III.) The minimum contribution to the flux I_B from particles whose most-probable pulse height is less than $h=12$ is 0.08 I_A'; this is simply the contribution arising from large ionization fluctuations of relativistic singly-charged particles. Subtraction of 0.08 I_A' from I_B yields I_B' (Table III) which we shall consider to represent the maximum slow-particle contribution to I_B.

The slow particles which, according to the fluctuation theory, have a chance ≥ 0.5 of producing a pulse in the interval $12<h<20$ are as follows:

(1) Protons incident from above the telescope with $208<E<253$ Mev.

(2) Protons incident from below the telescope with $235<E<348$ Mev.

(3) π mesons incident from below the telescope with $107<E<113$ Mev, where E is the telescope-entrance energy of the particles. The maximum combined flux of particles in these categories, given by $2\,I_B'$, is less than 8 percent of the total intensity in each altitude interval.

The slow singly-charged particles most likely to yield pulses in the relativistic α-particle range ($h>20$) are protons incident from below the telescope with energies in the region $208<E<235$ Mev. Inasmuch as this range is only $\frac{1}{4}$ as wide as the adjacent energy interval listed under item (2) above, it appears that the flux of slow protons yielding pulses which might be confused with α-particle pulses is less than 2 percent of I_{total}. This is quite small compared to the intensity of particles producing "α-candidate" pulses (C events); consequently, the slow protons will be left out of the consideration in the following section.

D. Relativistic α Particles

The calculated integral and differential pulse-height distributions for α particles of the geomagnetic cutoff energy (7 Bev per nucleon) are shown in Figs. 4 and 5, respectively. The ionization fluctuations of relativistic α particles are such that, with any reasonable assumption regarding the primary energy spectrum, less than 1 percent of those α particles which do not undergo local nuclear collisions should yield pulses with $h>48$. Thus, the events in the interval $20<h<48$ which are not shower-accompanied (C events) will be assumed to include all of the α particles which traversed the telescope without undergoing nuclear collisions. Subtraction from the C events of the expected contribution from large ionization fluctuations of relativistic singly-charged particles yields the flux values I_C' listed in Table III. Correction of the fluxes I_C' for the maximum percentage (38 percent) of α-particle pulses which could have occurred outside the C-interval by virtue of local nuclear interactions yields the α-particle flux upper limits I_C''. The probability of α-particle interaction in the telescope material was calculated with the aid of the cross section formula given in Sec. VI, B.

Curves representing the altitude variation of intensities I_C and I_C'' are plotted in Fig. 7. Inspection of the form of curve I_C'' indicates that the lower-altitude values must be far in excess of the actual α-particle flux. If the flux at 12 mm Hg were equal to the calculated upper limit, 39 sterad^{-1} m^{-2} sec^{-1}, and if the atmospheric absorbtion occurs as expected from the collision cross-section formula, the α-flux should be less than 1.0 sterad^{-1} m^{-2} sec^{-1} in the lowest altitude interval, as compared with the calculated upper limit 29 sterad^{-1} m^{-2} sec^{-1}.

If we assume that the spurious C events (i.e., those produced by particles other than α particles) are in equilibrium with the vertical flux of relativistic singly-charged particles in the interval 0–180 mm Hg—as is suggested by the approximate constancy of the ratio I_C/I_A in the interval 40 to 250 mm Hg—we obtain a revised α-flux value of 26 sterad^{-1} m^{-1} sec^{-1} at 12 mm Hg. The curve I_α in Fig. 7 is normalized to this value and is drawn with a slope corresponding to the expected atmospheric absorbtion of primary α particles (mean free path 44 g/cm^2). The zero-pressure intercept of curve I_α, 38 sterad^{-1} m^{-2} sec^{-1}, is believed a conservative upper limit for the primary α-particle flux at $\lambda=10°$.

[21] K. Anderson and J. R. Winckler (private communication).

It is interesting to note that if one computes from curve I_α the expected flux of proton fragments arising from the break up of vertically directed α particles, the computed flux accounts almost completely for the apparent transition (rapid change of slope) of the curve I_A in the top 50 g/cm^2 of the atmosphere. Proton fragments of heavier nuclei may also contribute to the indicated transition, but, according to existing data on the heavy primary flux and atomic weight distribution, fragments of these alone could not account for more than a small fraction of the effect noted.

Addition of the fluxes I_A'' and I_α yields the curve $(I_A''+I_\alpha)$ shown in Fig. 7. Comparison of this curve with I_{total} indicates that at 12 mm Hg at most 80 percent of the telescope counting rate can be attributed to vertically-incident relativistic protons and α particles. (The corresponding fraction at zero pressure, assuming the curves I_α and I_A'' to be extrapolated correctly, is 70 percent.) This gives a very strong indication that the telescope is triggered often at the "top of the atmosphere" by external showers or by particles incident from outside the telescope solid angle. It is interesting to note in this connection that the shower frequency (curve S, Fig. 7) has a very different altitude variation from the curve $(I_\alpha+I_A'')$ in the top 50 g/cm^2 of the atmosphere, and that the frequency of showers in this region is in excess of the maximum frequency of multiple-particle events that can arise from local nuclear interactions of telescope-oriented protons and α particles. This constitutes additional evidence of the presence of spurious telescope-triggering events and indicates that great care must be exercised in the interpretation of primary flux data obtained by means of telescopes having no shower protection.

VII. THE PROTON AND α-PARTICLE ENERGY SPECTRA

In Fig. 8 we have plotted the results of most of the existing α-particle flux measurements (see Introduction for methods and references) as a function of the theoretical geomagnetic cutoff energy at the location of each of the respective measurements.[22] The smooth curve A represents an integral energy spectrum of the form

$$N(\epsilon)=K/(1+\epsilon)^\gamma \qquad (2)$$

where ϵ is the primary-particle kinetic energy in Bev per nucleon and K and γ are assigned the values 420 sterad^{-1} m^{-2} sec^{-1} and 1.35 respectively. This spectrum agrees satisfactorily with the indicated He flux measurements and has the same form, except for the value of K, as the analytical expression chosen by Kaplon *et al.*[20] to represent the energy distribution of the primary nuclei with $Z\geqslant 10$.

[22] The upper and lower limits of experimental uncertainty on the author's point plotted in Fig. 8 are obtained, respectively, on the assumptions that *all* or *none* of the α particles which suffered nuclear collisions in the telescope gave rise to events other than those designated by C in the analysis.

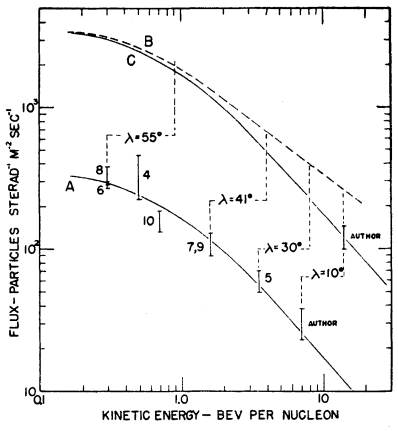

FIG. 8. Integral number-energy spectra of primary protons and α particles. The experimental data with the numerical indices (referring to footnote references) represent He flux measurements of other investigators. Curve A is a plot of the integral spectrum $N(\epsilon)=420(1+\epsilon)^{-1.35}$, where ϵ=primary energy in Bev/nucleon. Curve B is the "apparent" proton spectrum obtained by subtracting the α flux (curve A) from counter-telescope total-flux data. Curve C represents a spectrum of the form $N(\epsilon)=K(1+\epsilon)^{-1.35}$ fitted to the author's $\lambda=10°$ proton flux value.

The upper curve, B, in Fig. 8 represents an approximation to the primary proton energy spectrum deduced by subtraction of the estimated α-particle flux (curve A) from total flux values measured at various latitudes with G-M counter telescopes.[23] While the present total-flux measurement, corrected in a similar manner for the α-particle contribution, agrees precisely with curve B, the proton flux upper limit obtained from the pulse-height analysis (145 sterad^{-1} m^{-2} sec^{-1}) falls far below the curve.[24] The curve C shown in Fig. 8 represents a spectrum of the form of Eq. (2) with $\gamma=1.35$ and K adjusted to bring the curve into agreement with the present proton-flux estimate. Since curve C does not rise above curve A at low values of ϵ, it would appear that the proton spectrum could have the same form as that chosen to represent the He data, provided that the effects (showers and other spurious telescope-triggering events) which cause a departure between curve B and the present proton-flux value gradually become less important with increasing latitude.

The total cosmic-ray energy incident upon the atmosphere at various latitudes has been estimated from the ionization *vs* depth measurements of Bowen *et al.*[25] and also from the latitude variation of the total particle flux. The energy fluxes deduced by the two methods

[23] From a data compilation by Winckler, Stix, Dwight, and Sabin, Phys. Rev. **79**, 656 (1950).

[24] The upper and lower limits on the $\lambda=10°$ proton-flux value plotted in Fig. 8 are obtained by zero-pressure extrapolations of fluxes I_A'' and I_A' (Table III). The two limits correspond, respectively, to the assumptions that *all* or *none* of the protons which undergo interaction in the telescope give rise to events outside the A pulse-height interval.

[25] Bowen, Millikan, and Neher, Phys. Rev. **53**, 856 (1938) see interpretation presented by D. J. X. Montgomery, *Cosmic Ray Physics* (Princeton University Press, Princeton, 1949), p. 146.

differ by approximately a factor of 2, the ionization method yielding the smaller value. The energy flux calculated on the basis of the latitude effect depends critically on the form of the primary proton spectrum assumed for the region above 14 Bev—where accurate experimental data are lacking—and depends also upon the assumption that the counter telescopes measure directly the actual flux of primary particles. While the present data give no better information than has been available heretofore on the form of the particle spectra, there is strong evidence that the equatorial proton flux is approximately one-half that which has been assumed in the energy flux calculations based on the latitude effect. This observation suggests that the discrepancy noted above may arise from errors in particle flux measurements rather than from any serious oversight in the interpretation of the ionization *vs* depth data.

ACKNOWLEDGMENTS

The author wishes to thank Dr. W. F. G. Swann, Director of the Bartol Research Foundation, for his support and encouragement during all phases of this work. Among those who participated in the organization and execution of the balloon-flight operation, Project CHURCHY, were Lieutenant Commander Malcolm D. Ross of the Office of Naval Research, C. F. Merill of General Mills, Inc., and the officers and men of the U. S. Navy Ships Currituck, Rodman, and Ellison. The assistance of R. C. Pfeiffer and W. C. Porter, of the Bartol Research Foundation, is greatly appreciated.

PHYSICAL REVIEW VOLUME 96, NUMBER 5 DECEMBER 1, 1954

Production Spectra of Cosmic-Ray Mesons in the Atmosphere*

STANISLAW OLBERT
Massachusetts Institute of Technology, Laboratory for Nuclear Science, Cambridge, Massachusetts
(Received August 9, 1954)

Recent experimental data on the differential vertical intensities of μ mesons in the atmosphere make it possible not only to improve the original Sands' production spectrum of μ mesons but also to study its dependence on the geomagnetic latitude. It is shown that, for the residual ranges, R', between 100 g cm^{-2} and 6000 g cm^{-2}, the production spectrum may be approximated by an empirical formula of the type: $C(a+R')^{-\gamma}$ where C and γ are numerical constants practically independent of the geomagnetic latitude. The latitude dependence of the production spectrum is thus expressed through the parameter a which displays a monotonic decrease with increasing latitude. With numerical values of a, C, and γ, compatible with experimental data, the production spectrum of μ mesons is then used as a basis for the derivation of the differential and integral energy spectra of charged π mesons. The latitude dependence of the π-meson spectrum is linked to the geomagnetic cut-off of the primary cosmic radiation, which leads to some crude conclusions on the average multiplicity of π mesons produced in proton collisions with air nuclei. In particular, the dependence of the multiplicity on the primary energies between 2 and 13 Bev is studied in detail and compared with Fermi's statistical theory of π-meson production.

I. INTRODUCTION

THE original idea of M. Sands to introduce an empirical μ-meson spectrum at production[1] has been proven to be very useful in dealing with many problems concerning the mesonic components of cosmic rays in the atmosphere. The knowledge of this empirical production spectrum makes possible not only the computation of the vertical intensities of μ mesons at any desired altitude, but it also offers a basis for testing various theories of π-meson production in nucleonic collisions. The latter aspect is demonstrated, for example, by P. Budini and G. Molière in their review article in Heisenberg's *Kosmische Strahlung*[2] where the authors test Heisenberg's theory of multiple meson production.

Sands derived his production spectrum from early experimental data (partly his own, partly those of others) taken in the proximity of 45° geomagnetic latitude. Unfortunately, these data were then rather imcomplete and not quite suitable for Sands' task. Moreover, the values of the physical constants (like the rest mass or the lifetime of the μ meson) employed in Sands' calculations were, at the time, burdened by large experimental errors.

The purpose of this paper is, therefore, twofold: (a) to bring Sands' spectrum more up-to-date (Sec. II), (b) to extend its applicability to various geomagnetic latitudes (Sec. III). In addition, in Sec. IV we shall utilize the obtained latitude dependence of the μ-meson spectrum at production to study the relationship between the geomagnetic cut-off of the primary radiation and the integral energy spectrum of π mesons at production.

* Supported in part by the joint program of the U. S. Office of Naval Research and the U. S. Atomic Energy Commission.

[1] M. Sands, Technical Report No. 28, Laboratory for Nuclear Science, Massachusetts Institute of Technology, 1949 (unpublished); Phys. Rev. **77**, 180 (1950).

[2] *Kosmische Strahlung*, edited by W. Heisenberg (Springer-Verlag, Berlin-Göttingen-Heidelberg, 1953), second edition, p. 391 ff.